

UCLA

UCLA Previously Published Works

Title

Stickiness: A New Variable to Characterize the Temperature and Humidity Contributions toward Humid Heat

Permalink

<https://escholarship.org/uc/item/0v77m914>

Journal

Journal of the Atmospheric Sciences, 81(5)

ISSN

0022-4928

Authors

Ivanovich, Catherine C

Sobel, Adam H

Horton, Radley M

et al.

Publication Date

2024-05-01

DOI

10.1175/jas-d-23-0072.1

Copyright Information

This work is made available under the terms of a Creative Commons Attribution-NonCommercial-ShareAlike License, available at

<https://creativecommons.org/licenses/by-nc-sa/4.0/>

Peer reviewed

1 **Stickiness: A New Variable to Characterize the Temperature and**
2 **Humidity Contributions toward Humid Heat**

3
4 Catherine C. Ivanovich,^a Adam H. Sobel,^{a,b,c} Radley M. Horton,^b and Colin Raymond^{d,e}

5 ^a *Earth and Environmental Sciences, Columbia University, New York, NY*

6 ^b *Lamont-Doherty Earth Observatory, Columbia University, Palisades, NY*

7 ^c *Applied Physics and Applied Mathematics, Columbia University, New York, NY*

8 ^d *University of California Los Angeles, Los Angeles, CA*

9 ^e *Jet Propulsion Laboratory/California Institute of Technology, Pasadena, CA*

10
11 *Corresponding author: Catherine Ivanovich, cci2107@columbia.edu*

13

ABSTRACT

14 Extreme wet bulb temperatures (T_w) are often used as indicators of heat stress. However,
15 humid heat extremes are fundamentally compound events, and a given T_w can be generated
16 by various combinations of temperature and humidity. Differentiating between extreme
17 humid heat driven by temperature versus humidity is essential to identifying these extremes'
18 physical drivers and preparing for their distinct impacts. Here we explore the variety of
19 combinations of temperature and humidity contributing to humid heat experienced across the
20 globe. In addition to using traditional metrics, we derive a novel thermodynamic state
21 variable named "stickiness." Analogous to the oceanographic variable "spice" (which
22 quantifies the relative contributions of temperature and salinity to a given water density),
23 stickiness quantifies the relative contributions of temperature and specific humidity to a given
24 T_w . Consistent across metrics, we find that the occurrence of T_w sufficiently high to impact
25 human health tends to occur in the presence of anomalously high moisture, with temperature
26 anomalies of secondary importance. This widespread humidity-dependence is consistent with
27 the nonlinear relationship between temperature and specific humidity as prescribed by the
28 Clausius-Clapeyron relationship. Nonetheless, there are a range of humid-heat varieties
29 associated with moderate-to-high T_w . Stickiness allows a more objective evaluation of spatial
30 and temporal variability in this property of humid heat than traditional variables. In regions
31 with high temporal variability in stickiness, predictive skill for humid heat-related impacts
32 may improve by considering fluctuations in atmospheric humidity in addition to dry bulb
33 temperature.

34

35

SIGNIFICANCE STATEMENT

36 Extreme humid heat increases the risk of heat stress through its influence over humans'
37 ability to cool down by sweating. Understanding whether humid heat extremes are generated
38 more due to elevated temperature or humidity is important for identifying factors that may
39 increase local risk, preparing for associated impacts, and developing targeted adaptation
40 measures. Here we explore combinations of temperature and humidity across the globe using
41 traditional metrics and by deriving a new variable called "stickiness." We find that extreme
42 humid heat at dangerous thresholds occurs primarily due to elevated humidity, but that
43 stickiness allows for thorough analysis of the drivers of humid heat at lower thresholds,
44 including identification of regions prone to low- or high-stickiness extremes.

45 **1. Introduction**

46 Extreme humid heat events are climate extremes with important societal influence due
47 to their direct link to human and animal heat stress. Physiological research has suggested that
48 humid heat may pose additional risk to human health compared to dry heat due to its
49 influence over humans' thermoregulation efficiency (e.g., Mora et al. 2017; Parsons 2006;
50 Steadman 1979; Fanger 1970). While increased dry bulb temperatures alone can increase
51 rates of dehydration, over 75% of the heat dissipation by human bodies is associated with
52 evaporative cooling via sweating (Buzan and Huber 2020). The higher the ambient air
53 specific humidity, the more difficult it is for sweat to cool our bodies by evaporation; at
54 extremely high air temperatures, even a moderate amount of evaporative inhibition can cause
55 heat stress. Exposure to this type of heat stress is widespread across the globe, and has been
56 identified as one of the leading causes of death associated with climate extremes (Kovats and
57 Hajat 2008).

58 Differentiating between extreme humid heat and extreme dry heat is essential to
59 preparing for their individual impacts. Extreme humid heat may pose a higher risk to human
60 health and the potential for greater socioeconomic impacts than dry heat. In contrast, the
61 presence of humidity may diminish the effect of extreme heat on crop growth by reducing
62 vapor pressure deficit, for example in the United States Midwest (Schauberger et al. 2017;
63 Ting et al. 2023), and extreme dry heat has the potential to more strongly prime regions for
64 wildfires (Abatzoglou and Williams 2016; Bowman et al. 2009).

65 The physical drivers of dry and humid heat extremes are also somewhat distinct.
66 Extreme dry bulb temperatures tend to occur due to blocking events associated with
67 subsidence and clear sky conditions that lead to increased surface sensible heating
68 (Rothlisberger and Papritz 2023; Photiadou et al. 2014), aridity that prevents the cooling
69 effect of moisture evaporation (MacLeod et al. 2015), and urban heat island intensification
70 (Horton et al. 2016; Tan et al. 2010). Raymond et al. 2021 suggests on the other hand that
71 strong horizontal and vertical moisture fluxes, shallow boundary layers, nearby moisture
72 sources such as warm water bodies, and stability that inhibits moist convection are key
73 factors influencing extreme humid heat.

74 Due to these unique controlling mechanisms, the locations of the most intense
75 magnitudes of dry and humid heat are also distinct. Extreme temperatures occur primarily in
76 subtropical and lower-mid-latitude deserts, while hotspots of humid heat have more

77 geographic diversity (Rogers et al. 2021; Speizer et al. 2022). However, some locations do
78 experience both types of extremes. An example is South Asia, which experiences intense dry
79 heat extremes during the pre-monsoon season but where the increase in humidity associated
80 with monsoon wind and rain can intensify local humid heat conditions (Raymond et al. 2020;
81 Im et al. 2017).

82 As a multivariate extreme composed of the co-occurrence of elevated humidity and
83 temperature (Zcheischler et al. 2019), a given level of extreme humid heat can be generated
84 by various combinations of temperature and specific humidity. Extremes that are driven
85 largely by anomalous temperature or anomalous humidity have previously been described
86 throughout the literature as temperature- or humidity-dependent, respectively (Raymond et al.
87 2017; Wang et al. 2019; Ivanovich et al. 2022). Distinguishing between these varieties of
88 humid heat is especially important because while some adaptation measures, including
89 increasing cities' tree and grass cover, effectively reduce local dry bulb temperatures, the
90 simultaneous increases in humidity they cause may weaken their benefits in addressing heat
91 stress; furthermore, the efficacy of these adaptation strategies will themselves depend on the
92 ambient combination of temperature and humidity (Chakraborty et al. 2022). Additionally,
93 humid heat extremes of a given intensity created by high dry bulb temperatures in the
94 presence of some humidity have been shown in laboratory settings to be more detrimental to
95 human health than those with moderate temperatures and very high humidity (Vecellio et al.
96 2021). This indicates that regions in which extreme humid and dry heat co-occur may also be
97 the regions at highest risk for the most dangerous variety of heat stress.

98 Throughout the literature, the individual contributions from temperature and humidity
99 towards a region's experience of humid heat are defined on a scale relative to typical local
100 conditions (Raymond et al. 2017; Wang et al. 2019; Ivanovich et al. 2022). This has led to
101 definitions of temperature and humidity dependence that are difficult to compare from one
102 study to another. Given that substantial literature has developed on humid heat extremes,
103 having a consistent and universal method for evaluating how these extremes are physically
104 constituted from temperature and humidity is valuable for regional intercomparison, model
105 evaluation, and further theoretical development, as well as for heat stress preparedness
106 communication and adaptation.

107 In order to address this challenge, we first analyze the variability of humid heat
108 conditions within a set of climatologically diverse case study regions using traditional metrics
109 for temperature and humidity. We then derive a new thermodynamic state variable named

110 “stickiness,” apply it globally, and explore the additional insights it reveals. In Section 2, we
111 outline the methodologies used to evaluate the temperature and humidity dependence of
112 extreme humid heat. Section 3 describes the results of these analyses. Section 4 reflects on
113 the value, usability, and limitations of these different techniques, and provides suggestions
114 for pathways forward.

115

116 **2. Methods**

117 *2.1 Variables of analysis*

118 We select wet bulb temperature (T_w) as the primary humid heat variable for this
119 analysis. T_w describes the lowest temperature a parcel of air could reach if it were cooled and
120 moistened to the point of saturation by the adiabatic evaporation of liquid water at constant
121 pressure (e.g., Bohren and Albrecht 1998). T_w is thus a thermodynamic state variable which
122 provides a measurement of the efficiency of evaporative cooling, linking it directly to
123 humans’ experience of heat stress (Sherwood and Huber 2010). Particularly, T_w has been
124 shown to both exhibit thresholds at which survivability and livability are limited, dependent
125 upon physical characteristics of the individual experiencing the humid heat conditions
126 (Vecellio et al. 2022; Lu and Romps 2023; Vanos et al. 2023). We calculate T_w using the
127 Davies-Jones method (Davies-Jones 2008), which has been shown to more accurately capture
128 extreme values than other calculation methods (Buzan et al. 2015).

129 We explore the global and regional relationships between T_w , dry bulb temperature,
130 and humidity using standard variables: specific humidity, relative humidity, and saturation
131 deficit. In order to compute and analyze these variables, dry bulb temperature, dew point
132 temperature, and pressure data are retrieved from the HadISD station-based dataset (Dunn
133 2019). This dataset is produced by the Met Office Hadley Centre and records sub-daily
134 measurements from 8,486 stations. We retrieve the full historical data record for each station,
135 which is at most from year 1931 to year 2019 depending on individual station data
136 availability. For each station, we calculate the daily maximum T_w at each station location and
137 record the co-occurring temperature and specific humidity at this hour. We then use this data
138 to calculate the co-occurring relative humidity and saturation deficit. We do not perform any
139 preprocessing on the station data, relying on the Hadley Centre’s quality control methods
140 which include focus on the three variables required to calculate T_w (temperature, dewpoint,
141 and pressure) (Dunn et al. 2012). We note that the sampling frequency differences in a given

142 year or between stations could influence the recorded trends in daily maximum T_w and that
143 stations with lower sampling frequency are more likely to underestimate the magnitude of
144 daily maximum T_w . We conclude that these challenges should not influence our results
145 strongly as we do not compute trends and we are more interested in the conditions co-
146 occurring at a range of T_w thresholds rather than the absolute magnitude of daily maximum
147 T_w .

148 We then proceed to derive our new thermodynamic state variable — stickiness —
149 quantifying the temperature and humidity dependence of a given value of humid heat.

150

151 2.2 Thermodynamic state variable derivation

152 2.2.1 PRIMARY DERIVATION METHODS – WET BULB TEMPERATURE

153 After exploring information available from a wide range of diagnostics using
154 traditional variables, next we create a novel method for quantifying the relative temperature
155 and specific humidity dependence of humid heat by deriving a thermodynamic state variable
156 analogous to oceanographic spice, which we refer to as “stickiness.” Like spice, which
157 represents how salinity and temperature jointly affect the density of water, stickiness captures
158 the relative contributions of specific humidity and temperature to a given value of humid
159 heat. By design, stickiness varies most with fluctuations in temperature and specific humidity
160 at a given T_w , and least with changes in T_w itself.

161 Following the derivations for spice outlined by Flament (2002), we define a quantity
162 whose variations in a temperature-specific humidity space are maximally distinct from those
163 of T_w :

164

$$165 \quad \frac{\partial_T \tau}{\partial_T T_w} + \frac{\partial_q \tau}{\partial_q T_w} = 0 \quad \text{where } \tau \text{ is stickiness and } \partial_T \tau \text{ refers to } \frac{\partial \tau}{\partial T} \quad (1)$$

166

167 where T is temperature, q is specific humidity, T_w is wet bulb temperature, and τ is stickiness.

168 Stickiness is computed here as a polynomial equation, up to degree three in both
169 temperature and specific humidity, constructed to satisfy equation (1) as described below. T_w
170 isopleths are close to linear in a temperature-specific humidity space, and degree three is thus
171 sufficient to capture this structure (Figure 4). Sensitivity to increasing the degree of the

172 polynomial in each variable is negligible (not shown). The polynomial equation for stickiness
 173 can thus be expressed as:

174

$$175 \quad \tau(T, q) = - \sum_{i=0}^3 \sum_{j=0}^3 b_{ij} T^i q^j \quad (2)$$

176

177 where b_{ij} refers to coefficients of term ij . This final derived polynomial equation allows for
 178 the calculation of stickiness given inputs of dry bulb temperature and specific humidity.

179 We then compute the coefficients of the polynomial equation for stickiness
 180 numerically by performing a bound-constrained function minimization on an associated mean
 181 squared error. This mean squared error is defined as:

182

$$183 \quad \epsilon^2 = \lambda_1 \iint dT dq \left[\frac{\partial_T \tau}{\partial_T T_w} + \frac{\partial_q \tau}{\partial_q T_w} \right]^2 + \lambda_2 \iint dT dq \left[\frac{\partial_T \tau}{\partial_T T_w} - 1 \right]^2 \quad (3)$$

184

185 where the first and second term represent the geometric and scaling constraints for stickiness,
 186 respectively, indicating that stickiness should be invariant for all geometric transforms and
 187 scaling changes allowed in the prescribed temperature-specific humidity domain. The second
 188 term also provides units to stickiness, determining that stickiness scales as T_w does with
 189 temperature and possesses units of degrees Celsius. The λ_1, λ_2 are weights, set at 0.8 and
 190 0.2, respectively. These derivation methods are relatively insensitive to changes in these
 191 weightings (not shown), and thus these values are selected following Flament (2002), to place
 192 greater dependence on the geometric constraint between the stickiness isopleths and the T_w
 193 isotherms over that of the scaling constraint. For more information, see Flament (2002).

194 The Nelder-Mead method using the Simplex algorithm is selected for the
 195 minimization (Nelder and Mead 1965; Wright 1996), with a tolerance for termination at 10^{-8}
 196 and a maximum of 100,000 function evaluations. This minimization search is executed on a
 197 temperature-specific humidity grid ranging from 25°C to 50°C and 0 g/kg to 20 g/kg (with a
 198 resolution of 0.05°C and 0.04 g/kg), calculating T_w assuming a constant 1000 hPa surface
 199 pressure. Assuming a constant surface pressure reduces the dependence of stickiness upon
 200 pressure fluctuations in a given location. The elevations of global station locations used in

201 this analysis range from -350 m (Ghor El Safi, Jordan) to 4,736 m (T'u-Ko-Erh-Ho-Kung,
202 China). However, the temperature-specific humidity space in which we conduct our
203 derivation covers most of the tropics and mid-latitude warm seasons, typically close to the
204 1000 hPa surface pressure selected. Further, we perform a sensitivity test in order to evaluate
205 the effect of neglecting this pressure dependence and find that the resulting equation for
206 stickiness is valid for surface pressures greater than 900 hPa (Figure S1), encompassing
207 virtually all high-humid heat locations and events. Because extreme humid heat and its
208 impacts attenuate rapidly with increasing elevation (decreasing pressure) (Raymond et al.
209 2022), we deem this to be a relatively minor caveat.

210 The derivation methods described are agnostic to the absolute magnitude and sign of
211 stickiness. To aid in interpretability, the negative sign on the right hand side of equation (2)
212 represents our chosen sign convention, where positive values of stickiness reflect higher
213 humidity dependence. Further, the final equation for stickiness is shifted so that the zero
214 value is equal to the mean conditions across all HadISD station locations (time averaging the
215 full data record for each individual station and then taking the mean over all stations).
216 Positive values of stickiness thus represent higher than average humidity dependence, while
217 negative values represent higher than average temperature dependence. Unlike for dry bulb
218 temperature, a 0°C value of stickiness is unrelated to freezing conditions. Due to the
219 dominance of station density in Europe and North America, we perform a sensitivity test for
220 this shift in the total magnitude of stickiness. We first average mean stickiness across 30°
221 latitudinal bands (e.g., 0-30°, 30-60°, and 60-90° in the Northern and Southern Hemispheres)
222 and then take a weighted average across these six values based on the number of stations in
223 each band (Figure S2). This second method results in a global mean stickiness value just
224 0.6°C higher than the method using a simple mean. Given the mean standard deviation in
225 stickiness during local summer across the globe is 1.3°C, the difference between these
226 methodologies is relatively small and should not be expected to influence the presented
227 results' interpretation.

228 Executing these derivation methods generates a polynomial equation for stickiness in
229 terms of temperature and specific humidity, with the coefficients of expressed in Table 1.
230 Stickiness is measured in degrees Celsius due to the derivation's foundation on T_w , also with
231 units of degrees Celsius. Worked examples highlighting the relationships between
232 temperature, specific humidity, T_w , and stickiness are outlined in Table 2. We see, for
233 example, that under annual mean conditions at a tropical location (here we select Jakarta,

234 Indonesia for illustration), increasing the dry bulb temperature by 1°C while holding specific
 235 humidity and pressure constant results in a decrease in stickiness of 2.2°C and an increase in
 236 T_w of 0.3°C. Under the same initial conditions, increasing specific humidity by 1 g/kg leads
 237 to an increase in stickiness of 0.6°C and an increase in T_w of 0.6°C.

238

Coefficients of term $T^i q^j$		j			
		0	1	2	3
i	0	-1.200	775.269	-7740.957	-7186.001
	1	-0.302	-3.086	238.012	-429.814
	2	-0.00178	0.4987	-24.017	283.672
	3	0.000027	-0.00702	0.367	-5.094

239 **Table 1:** Stickiness equation coefficients for T in degrees Celsius and q in kg/kg.

240

Initial Conditions	Change Applied	Resulting Conditions
T = 28.4 °C q = 18.2 g/kg p = 1009 hPa stick = 2.9 °C T_w = 24.7 °C	Holding q constant, increase temperature by 1 °C to: T = 29.4 °C	stickiness = 0.7°C (-2.2°C) T_w = 25.0°C (+0.3°C)
	Holding T constant, increase specific humidity by 1 g/kg to: q = 19.2 g/kg	stickiness = 3.5 °C (+0.6°C) T_w = 25.3°C (+0.6°C)
	Holding stickiness constant, increase temperature by 1 °C to: T = 29.4 °C	q = 18.6 g/kg (+0.4 g/kg) T_w = 25.2°C (+0.5°C)
	Holding stickiness constant, increase specific humidity by 1 g/kg to: q = 19.2 g/kg	T = 30.8°C (+2.4°C) T_w = 25.9°C (+1.2°C)

	Holding T_w constant, increase temperature by 1 °C to: T = 29.4 °C	$q = 18.0 \text{ g/kg}$ (-0.2 g/kg) stickiness = 2.3 °C (-0.6°C)
	Holding T_w constant, increase specific humidity by 1 g/kg to: q = 19.2 g/kg	$T = 26.4^\circ\text{C}$ (-2.0 °C) stickiness = 4.0°C (+1.1°C)

241 **Table 2:** Worked examples of tradeoffs between temperature, specific humidity, T_w , and stickiness. Initial
242 conditions reflect a set of typical tropical conditions, here chosen as annual mean conditions at 1pm in
243 Jakarta, Indonesia. Pressure (p) constant in all scenarios.

244

245 The derivation methods described in this section can be applied based on any humid
246 heat metric measuring the combination of temperature and humidity, such as Humidex
247 (Masterton and Richardson 1979). We have applied the same computational derivation
248 methods to Humidex, for reference, and the results of this derivation are shown in Table S1
249 and Figure S3. The code used for these numerical derivations will be publicly available on
250 Github for users interested in applying these methods to their humid heat metric of choice.
251 We have also applied these methods for moist static energy and compared our results to an
252 analytic derivation in the following section.

253

254 2.2.2 SUPPLEMENTAL ANALYTICAL DERIVATION METHODS – MOIST STATIC 255 ENERGY

256 While moist static energy (MSE) does not have the same direct link to heat stress as
257 T_w and is not explicitly related to the socioeconomic impacts of humid heat, these two
258 variables are closely related to one another thermodynamically and should be expected to
259 behave similarly. With this in mind, we construct a version of stickiness based on MSE.
260 Because it is analytically tractable, a derivation for stickiness based on MSE provides a
261 simpler illustration of the concept than the numerical derivation method described above,
262 although the latter is necessary for application to T_w . Moist static energy can be expressed as:

263

$$264 \quad MSE = C_p T + gz + L_v q \quad (4)$$

265

266 where C_p is the specific heat capacity, g is the gravitational constant, z is the vertical height,
267 and L_v is the latent heat of vaporization. At the surface ($z = 0$), this expression simplifies to a
268 linear combination of temperature and specific humidity:

269

$$270 \quad MSE = C_p T + L_v q \quad (5)$$

271

272 In this case, deriving stickiness as a variable whose changes in temperature-specific humidity
273 space are maximally distinct from those of our humid heat variable – now surface MSE – can
274 be executed analytically, yielding the result:

275

$$276 \quad \tau_{MSE} = C_p T - L_v q \quad (6)$$

$$277 \quad \text{or} \quad \tau_{MSE} = -C_p T + L_v q \quad (7)$$

278

279 where equation (7) has been assigned the same sign convention described in the numerical
280 derivation above for T_w , with high (low) stickiness reflecting humidity-dependence
281 (temperature-dependence).

282 We use this MSE-based derivation in order to help clarify the goal of our numerical
283 derivation, as well as to check its accuracy against the analytical solution. Indeed, the
284 solutions are in close agreement (Figure S4). We present a second set of results for the MSE-
285 based derivation in the supplement, but focus on the T_w -based definition in the main text due
286 to our motivation to capture patterns relevant to societal impacts. We find similar overall
287 conclusions from each derivation method (Figures S18 and S19).

288

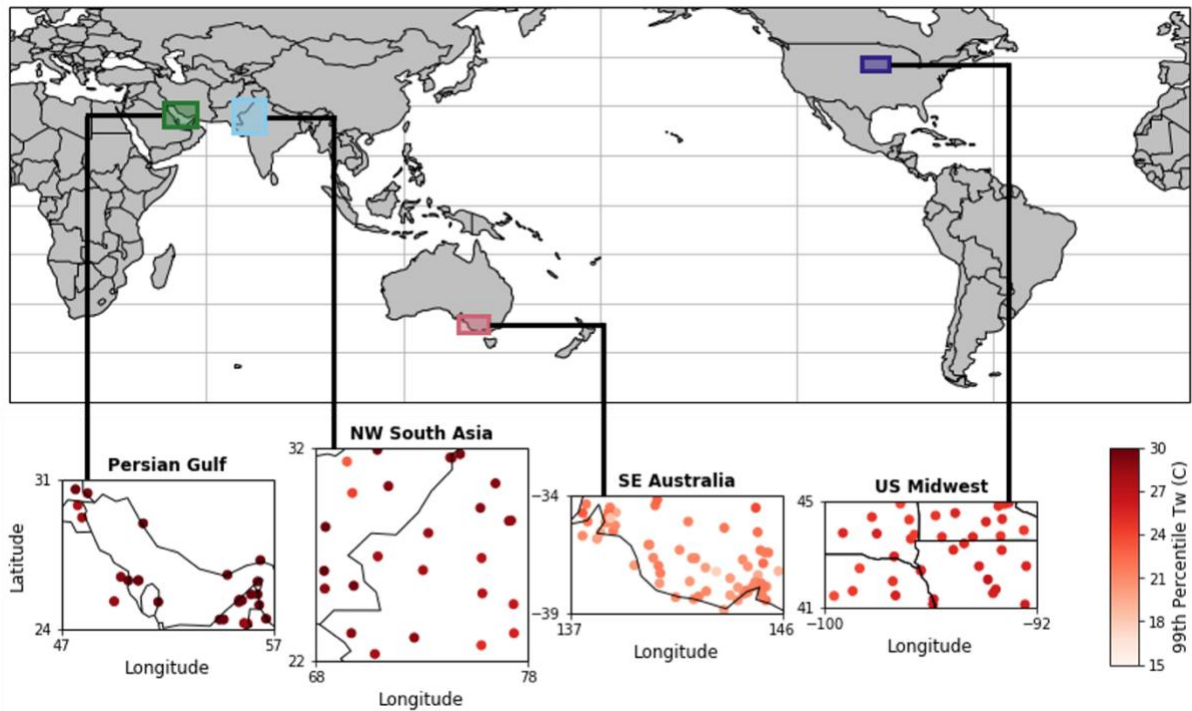
289 *2.3 Regional comparisons*

290 We explore the relationships between temperature, humidity, and humid heat by
291 comparing patterns in existing heat and humidity variables identified in four climatologically
292 distinct regions. These regions are the Persian Gulf (45-60 °E, 20-36 °N, restricted to stations
293 with a 99th percentile T_w above 28°C), northwestern South Asia (68-78 °E, 22-32 °N),
294 southeastern Australia (141-154 °E, 28-39°S), and the United States Midwest (92-100 °W,

295 41-45 °N) (Figure 1). The first two regions (“Persian Gulf” and “NW South Asia”) were
296 selected based on their historical propensity for extreme humid heat (Raymond et al. 2021,
297 Rogers et al. 2021; Raymond et al. 2020). In both of these locations, extreme humid heat
298 events depend strongly on moisture modulation yet are associated with unique large-scale
299 meteorological patterns across distinct geographies (Pal and Eltahir 2016; Im et al. 2017;
300 Monteiro and Caballero 2019; Mishra et al. 2020; Ivanovich et al. 2022). Southeastern
301 Australia (“SE Australia”) was selected to provide contrast to these humid heat hotspots, due
302 to its Mediterranean climate with lower summer humidity. The United States Midwest (“US
303 Midwest”) was selected due to the complex influence of cropland on humid heat in the area,
304 shown to increase local humidity but decrease local dry bulb temperatures (Coffel et al. 2022;
305 Ting et al. 2023; Mueller et al. 2016). We note that all regional analyses in this study treat
306 daily scale station measurements as individual data points, rather than averaging conditions
307 across stations. The aggregation of these stations may complicate interpretation due to the
308 potential grouping of diverse locations into the boxed boundaries described above. Such
309 limitations motivated the additional selection criterion for the Persian Gulf region in order to
310 avoid dry, mountainous locations in Iran which experience drastically different climatologies
311 than the rest of the stations in the region. Single station scale analyses were also performed
312 when necessary to help discern the source of variability in identified patterns.

313

314



316

317 **Figure 1:** HadISD station locations included in regional analyses, colored by 99th percentile daily
 318 maximum T_w (full year). Four boxed regions of interest are referred to as Persian Gulf, NW South Asia,
 319 SE Australia, and US Midwest.

320

321 3. Results

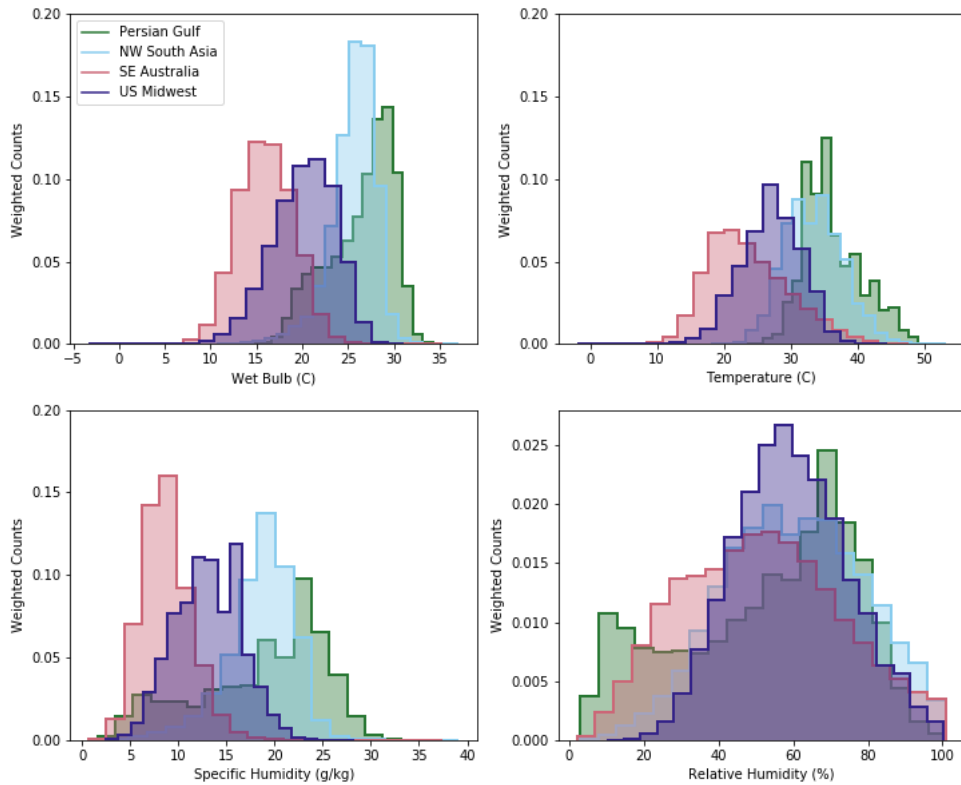
322 3.1 Exploration of temperature and humidity combinations through traditional variables

323

324 Our four case study regions experience varying intensities of humid heat and distinct
 325 mechanisms which bring about local humid heat extremes. Firstly, these regions exhibit
 326 contrasting distributions in temperature, humidity, and T_w (Figure 2). Each of the four
 327 regions has a unimodal temperature distribution. This is also true for T_w , specific humidity,
 328 and relative humidity in all regions except for the Persian Gulf, which has a bimodal
 329 distribution in these three variables. The areas surrounding the Persian Gulf are very dry
 330 throughout the Northern Hemisphere summer, but the advection of marine air through strong
 331 sea breezes and synoptic scale meteorological conditions increases local humidity and under
 332 certain conditions can drive T_w into dangerous thresholds (Ivanovich et al. 2022; Raymond et
 333 al. 2021; Pal and Eltahir 2016; Xue and Eltahir 2015). We note that removing the
 334 requirement that all stations in the Persian Gulf region exhibit a 99th percentile T_w above 28

335 °C increases the spread of these distributions in specific humidity, relative humidity, and T_w
 336 (not shown), but that the bimodal distributions is retained for all thresholds tested between
 337 25-30°C. Further, this bimodality is consistent across the individual station locations selected
 338 for this region, and an example using a station in Dammam, Saudi Arabia is plotted in Figure
 339 S5 for reference.

340



341

342 **Figure 2:** Histograms of T_w , dry bulb temperature, specific humidity, and relative humidity in the four
 343 regions of interest. Shown for local summer season (JJA for the Persian Gulf, NW South Asia, and the US
 344 Midwest; DJF for SE Australia). Note smaller y-axis range for fourth panel in order to visualize shape of
 345 the broader distributions.

346

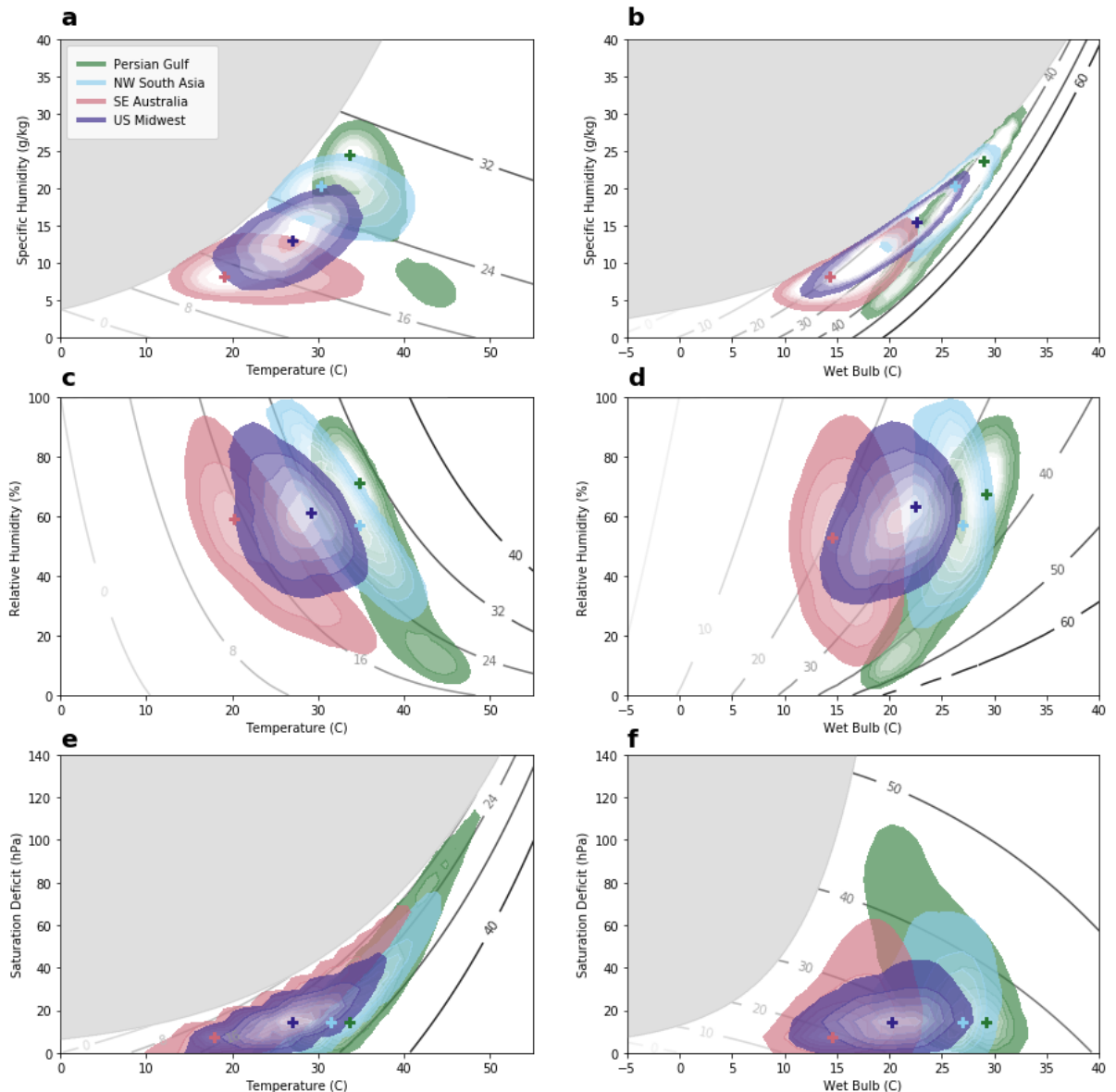
347 To visualize the full record of daily scale station data within each region, we plot the
 348 dry and wet bulb temperature at the hour of recorded daily maximum T_w against a variety of
 349 co-occurring humidity metrics: specific humidity, relative humidity, and saturation deficit.
 350 We find that locally extreme dry bulb temperatures can occur at a range of specific
 351 humidities, although consistently low relative humidities (Figure 3a, 3c). In NW South Asia,
 352 elevated temperatures are associated with changes in specific humidity which in combination
 353 generate a relatively small range in T_w compared to the other three regions. This indicates a
 354 tendency for compensatory effects, whereby temperatures vary more than specific humidity

355 and variations in specific humidity tend to partially offset those in temperature, possibly
356 indicative of the simultaneous cooling and moistening effect of evaporation of soil moisture
357 or surface water. In the US Midwest, high temperatures are associated with high specific
358 humidities, suggesting a larger potential for elevated temperature and specific humidity to co-
359 occur, with both factors contributing to extreme T_w . The most extreme T_w days in SE
360 Australia occur at moderately high temperatures (roughly 35°C) when the air is virtually
361 saturated (Figure S6). A bimodal distribution is again evident in the Persian Gulf, with the
362 majority of days at high temperatures and high specific humidities, which contrasts with a
363 smaller cluster of extreme temperature dry days. In all four regions, the highest recorded T_w
364 are associated with the highest recorded specific humidity conditions (Figure 3b). Further, the
365 distribution of conditions in each region shows that increases from locally moderate to
366 extreme T_w cross few temperature isotherms, suggesting that extreme humid heat conditions
367 tend to be humidity dependent.

368 We also observe that the most extreme temperatures are associated with a small range
369 of very low relative humidities in three of the regions. The relative humidities that occur
370 with extreme T_w apparently differ more widely than those that occur with extreme
371 temperatures. In the Persian Gulf, NW South Asia, and SE Australia, increasing temperatures
372 are closely associated with decreasing relative humidities, hewing fairly closely to lines of
373 constant T_w (Figure 3c). At locally high T_w thresholds, the distributions in NW South Asia
374 and SE Australia cross many temperature isotherms (Figure 3d), indicating that extreme
375 temperatures are not a necessary component to generating humid heat extremes in these
376 regions. The associated relative humidities also vary substantially, though still within the
377 upper half of the local distribution (Figure 3d). The bimodal structures in the relationships
378 between relative humidity and both temperature and T_w are again clear in the Persian Gulf,
379 delineating between days which are hotter and drier versus cooler and more moist. NW South
380 Asia experiences most summer days in a high relative humidity environment, while the
381 relative humidity and T_w conditions in the US Midwest are lower and more consistent than
382 the other three regions.

383 While extreme T_w can exhibit a slightly larger range in saturation deficit than extreme
384 dry bulb temperatures, this difference is not as pronounced as for relative humidity. The
385 highest recorded temperatures in each region are associated with the highest recorded
386 saturation deficits (Figure 3e). Further, changes in temperature are compensated by changes
387 in saturation deficit which keep T_w at a roughly constant intensity. Extreme T_w in the Persian

388 Gulf, SE Australia, and the US Midwest are limited to those days very close to saturation
389 (Figure 3f). In NW South Asia, in contrast, extreme T_w span a range of saturation deficits and
390 cross many dry bulb temperature contours. The T_w in the US Midwest and SE Australia tend
391 to be lower with small ranges in saturation deficits, suggesting both that temperature and
392 specific humidity tend to fluctuate jointly in these regions, and that an absence of very high
393 temperatures may limit how large saturation deficits can be. In each panel of Figure 3, the
394 strong relationship between certain heat and humidity metrics is evident. Particularly, relative
395 humidity and saturation deficit depend strongly on temperature, which is reflected in the
396 same correlation sign between these variables in the four case study regions. Conversely,
397 while retaining some dependence on temperature, T_w is much more sensitive to specific
398 humidity than to the other two humidity variables, sharing a consistent increase with specific
399 humidity that is not observed with relative humidity or saturation deficit.



400
 401 **Figure 3:** Daily temperature and humidity conditions for historical data record over all stations in each
 402 region. Temperature (left column) and T_w (right column) compared to specific humidity (top row), relative
 403 humidity (middle row), and saturation deficit (bottom row). Shaded contours indicate Gaussian kernel
 404 density estimation of conditions during daily maximum T_w for each region (with colored cross at the
 405 distributions' center); gray contours indicate T_w (left column) and dry bulb temperature (right column)
 406 isotherms. Gray shading indicates conditions producing supersaturated air. Shown for local summer season
 407 (JJA for the Persian Gulf, NW South Asia, and the US Midwest; DJF for SE Australia).

408

409 Overall, we conclude that while high dry bulb temperatures can occur at a range of
 410 moisture levels, the occurrence of extreme humid heat is much more limited to a narrow
 411 range of anomalous humidity (most clearly when measured by specific humidity). However,
 412 there are a small fraction of days associated with highly elevated dry bulb temperatures in the
 413 presence of moderate humidity that together causes extreme T_w . The various combinations of
 414 these standard variables, in multiple plots made from long-term station records in each

415 region, allows us to draw these conclusions with some confidence and nuance. However,
416 extending this analysis to a global scale by recreating these plots for all station locations
417 would be intractable. The lack of a global benchmark for meaningfully comparing disparate
418 temperature and humidity combinations adds another complication. We could thus hope for a
419 more direct route to these conclusions, and especially one that allows us to compare the
420 humidity or temperature dependence of humid heat in locations around the world more
421 straightforwardly and objectively. Towards this end, we use the following section to explore
422 the use of stickiness, whose derivation was outlined above.

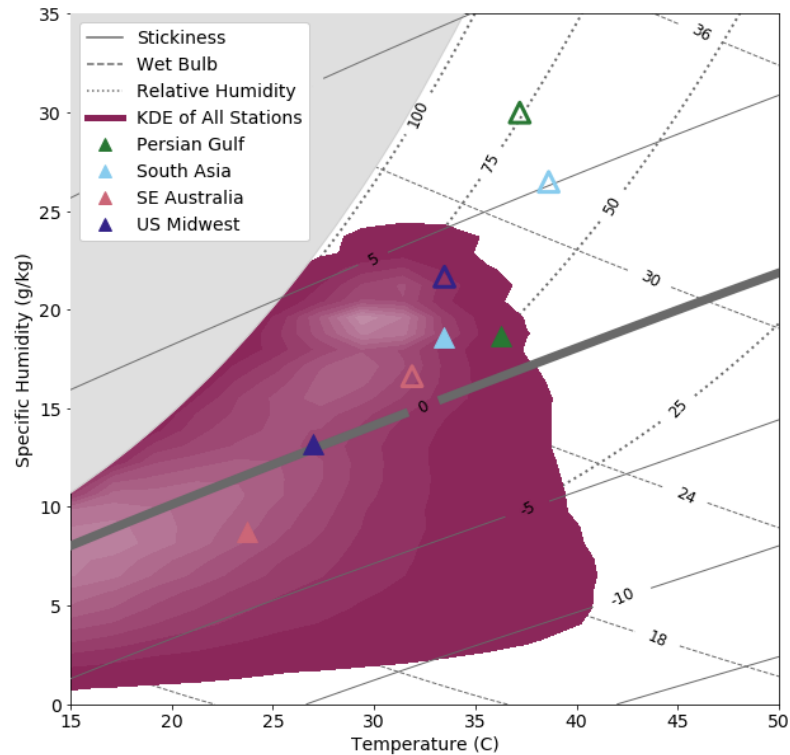
423

424 *3.2 Stickiness derivation results and analysis*

425 We derive a thermodynamic state variable, stickiness, which varies most with
426 fluctuations in dry bulb temperature and specific humidity and is least correlated with T_w .
427 Our methods generate a consistent and globally applicable scale with which to compare the
428 temperature-vs-specific humidity contributions towards a given intensity of T_w .

429 Stickiness is constructed so that the mean value over all stations' historical records is
430 0°C , and we observe that a large fraction of conditions observed on Earth occur around 0°C
431 (Figure 4). The mean conditions in the four case study regions are also close to this zero
432 value, while their 99th percentile T_w conditions are all at positive stickiness. This supports
433 the conclusion reached by previously published literature that extreme humid heat tends to be
434 humidity dependent (e.g., Raymond et al. 2020, Lutsko et al. 2021). This pattern is also
435 supported by our physical understanding of the relationship between temperature and specific
436 humidity. Due to the Clausius-Clapeyron relationship, higher dry bulb temperatures are
437 associated with the ability for air to experience exponentially higher specific humidity before
438 reaching saturation. This allows the potential magnitude of local specific humidity variations
439 to increase non-linearly with temperature, suggesting that the contributions of humidity
440 fluctuations to extreme humid heat may be greater than those of dry bulb temperature
441 fluctuations. Similarly, it implies certain seasonal and geographic patterns of stickiness as
442 explored in later sections. As the climate continues to warm, higher latitudes will likely see
443 greater variability in specific humidity along with that in temperature (Lutsko et al. 2021) and
444 occasional high stickiness conditions may progress further poleward. Additionally,
445 comparing the stickiness contours in Figure 4 with the relative humidity and saturation deficit

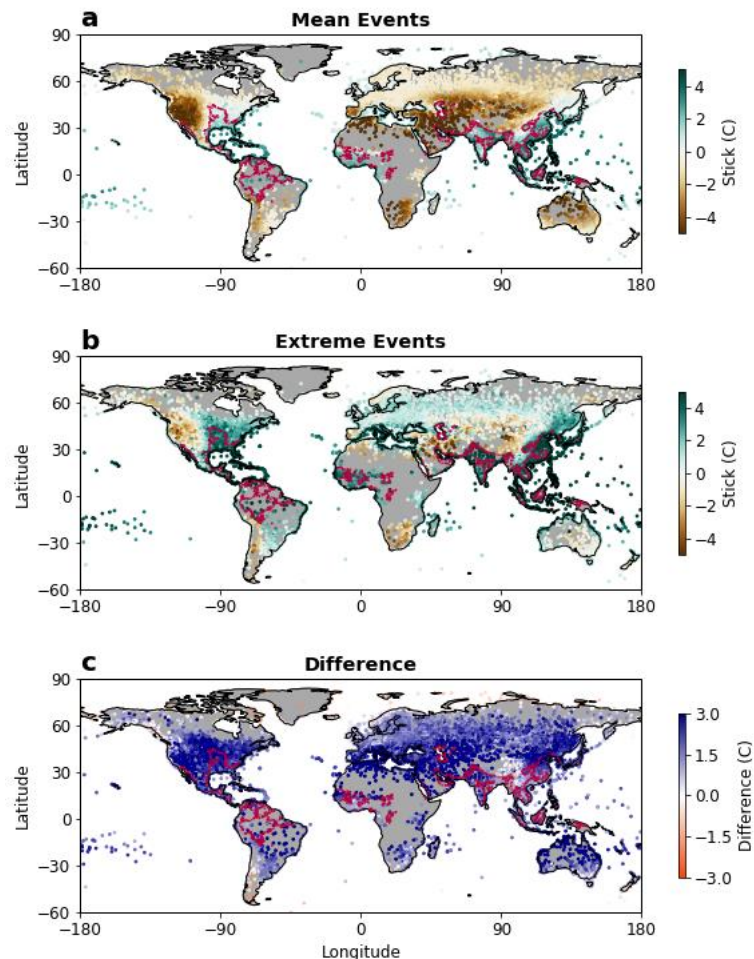
446 contours in Figure 3, stickiness does not exhibit the same non-linearities at extreme
 447 temperatures. Stickiness may thus be a useful diagnostic at very high and low temperatures.



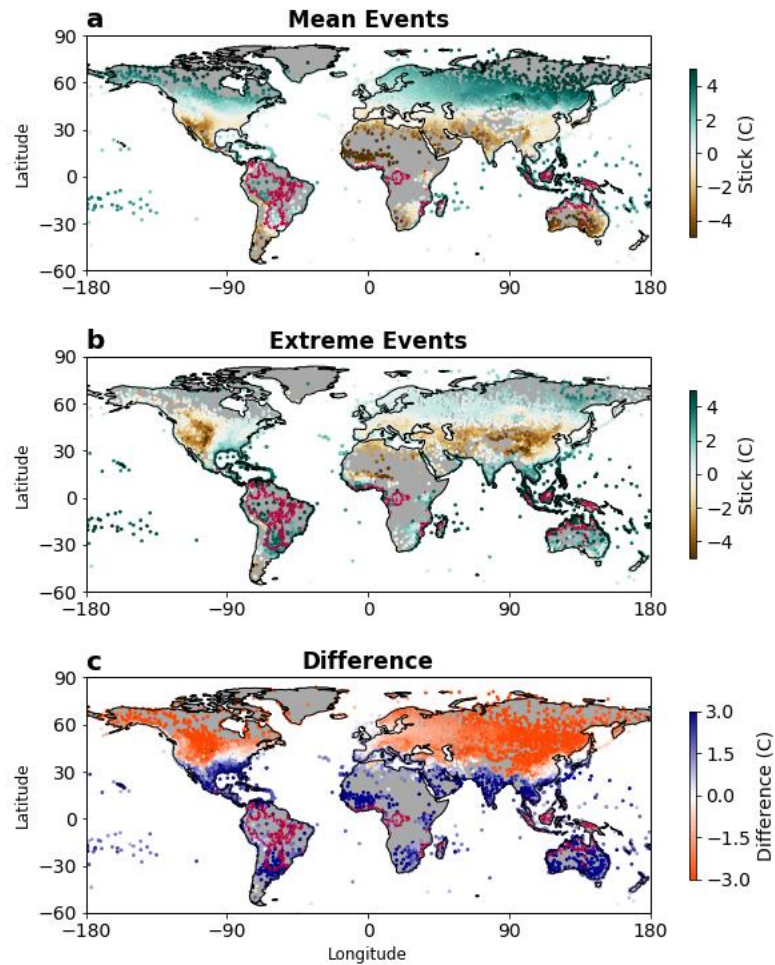
448
 449 **Figure 4:** Families of T_w isotherms and stickiness isopleths. Zero value calculated based on mean
 450 stickiness conditions associated with all station locations (full year data), as shown by the magenta
 451 shading. Grey shading indicates supersaturated conditions. Filled (open) triangles indicate regional mean
 452 stickiness conditions on all days in the year (99th percentile T_w days). Dotted grey lines indicate relative
 453 humidity isopleths.

454
 455 Stickiness is a single variable that measures the spatial variability of global humid
 456 heat temperature-vs-humidity dependence. During the hour of recorded daily maximum T_w
 457 for all days in each station record, high stickiness is found commonly in coastal regions
 458 (Figures 5a and 6a). Regions with monsoon climates also exhibit higher stickiness in rainy
 459 seasons than in dry seasons. For example, South Asia tends to experience higher stickiness
 460 during the June-August (JJA) season than the December-February (DJF) season. The lowest
 461 values of stickiness under both mean and extreme conditions are at high elevation, including
 462 the regions near the Andes Mountains, the Tibetan Plateau, and the Rocky Mountains.
 463 Summer patterns in stickiness for the Northern and Southern Hemispheres (when local T_w are
 464 more intense) are distinct. Namely, mean stickiness conditions in the Southern Hemisphere
 465 are not nearly as high as those in the Northern Hemisphere, consistent with the observation

466 that there is higher mean specific humidity in the Northern Hemisphere compared to the
 467 Southern Hemisphere (Dai et al. 2006). Further, high stickiness under mean T_w extends to
 468 much higher latitudes on the eastern coast of North America and Asia during JJA than do
 469 those in the Southern Hemisphere during DJF (Figure 5a and 6a), but these stickiness values
 470 decrease rapidly towards the west into the interior of each continent. Additionally, a higher
 471 fraction of tropical Northern Hemisphere stations exhibit positive stickiness under mean
 472 conditions during DJF than do tropical Southern Hemisphere stations during JJA. The highest
 473 temporal standard deviation in stickiness tends to occur in semi-arid coastal regions (Figure
 474 S14a and S15a). These include southeastern Australia, South Africa, and the Sahel, each of
 475 which experiences large interannual climate variability including strong influences of the El
 476 Niño Southern Oscillation (ENSO) phenomenon. Stickiness also exhibits high variability in
 477 extreme humid heat hotspots, where the mean values are also large.



478
 479 **Figure 5:** Global maps of mean stickiness during the hour of daily maximum T_w at each station location
 480 based on subset of the data record during JJA season: a) data from all days in each station record, b) data
 481 from 99th percentile T_w days, c) difference between these two maps (b - a). Red contours indicate regions
 482 with 99th percentile T_w above 27 °C (based on JJA season, ERA5 gridded reanalysis data).



483

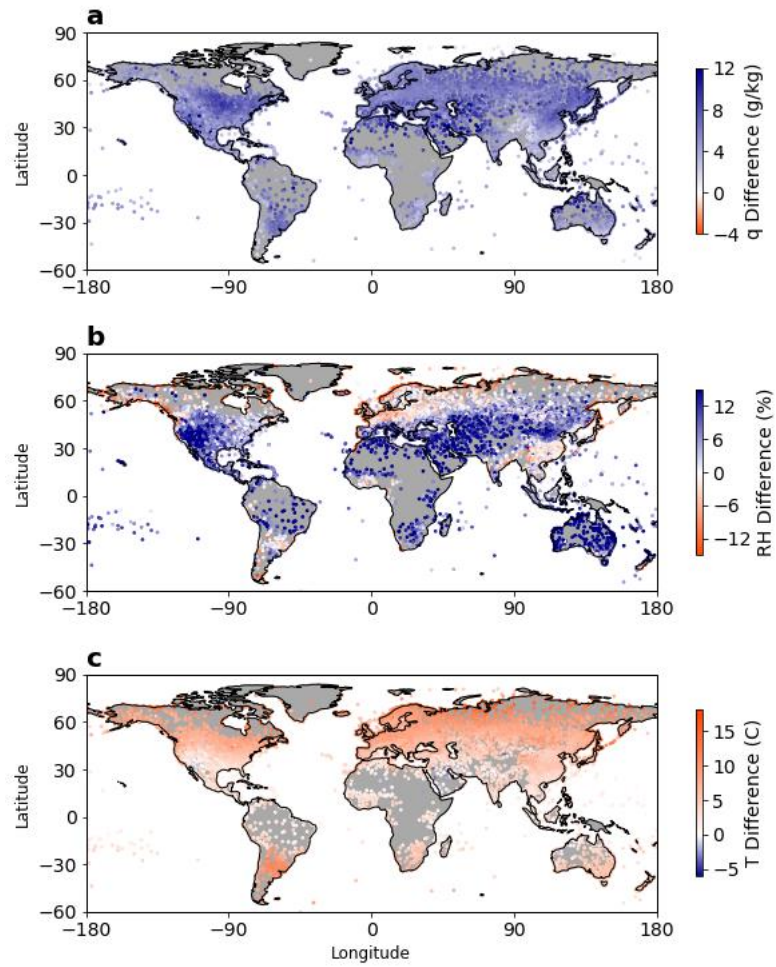
484 **Figure 6:** Global maps of mean stickiness during the hour of daily maximum T_w at each station location
 485 based on subset of the data record during DJF season: a) data from all days in each station record, b) data
 486 from 99th percentile T_w days, c) difference between these two maps (b - a). Red contours indicate regions
 487 with 99th percentile T_w above 27 °C (based on DJF season, ERA5 gridded reanalysis data).

488

489 Stickiness is higher during extreme T_w events than during mean conditions at most
 490 stations around the globe during the local summer season. In fact, many stations have never
 491 reached a locally extreme T_w under low stickiness conditions, and this is particularly true in
 492 regions where the 99th percentile T_w threshold is sufficiently high to impact human health,
 493 such as the Persian Gulf, South Asia, the Sahel, and the Amazon basin (Figure S16). Around
 494 the globe, stickiness is constrained to positive values during high intensity humid heat days,
 495 while there is a larger range of stickiness during more moderate humid heat conditions
 496 (Figure S17). At the same time, some regions do maintain their overall temperature
 497 dependence (low stickiness) even on locally extreme T_w days. These stations include those
 498 located in the western United States, the Sahara, Iran, and Chile and are primarily in
 499 continental-interior locations which have no pathway to advect warm and humid air from a

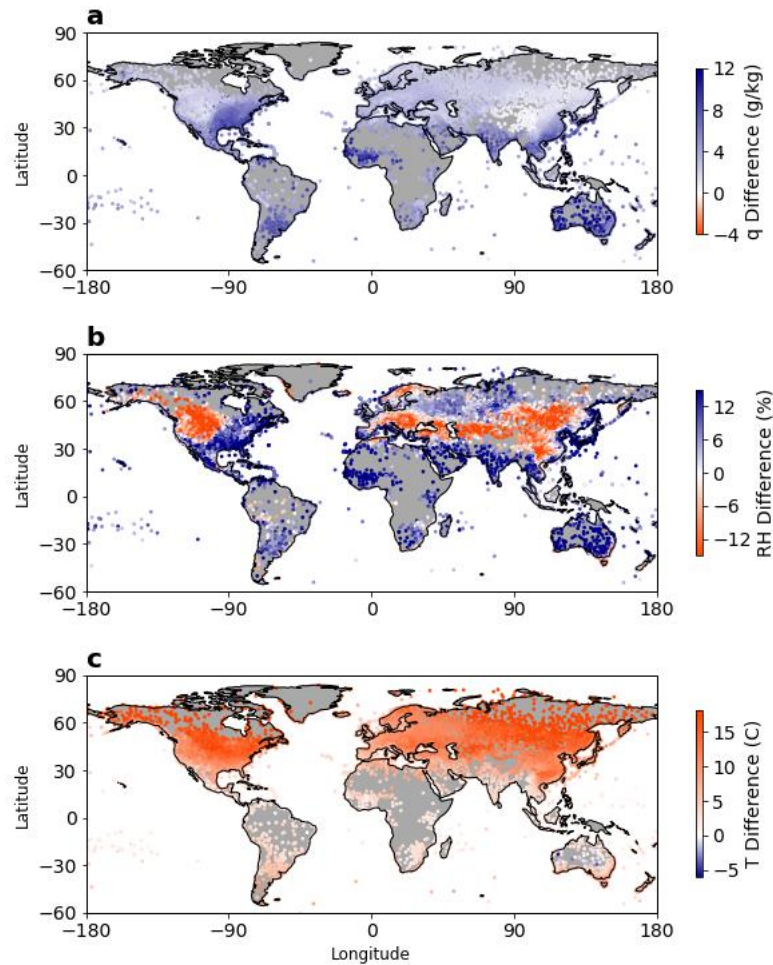
500 surrounding water body or region of high soil moisture. However, for a subset of near-coastal
501 stations—for example in Alaska and on the Scandinavian coast — the low stickiness may be
502 a consequence of the cool sea surface temperatures offshore, and could change as those
503 temperatures warm. While nearly all stations exhibit an increase in stickiness on extreme T_w
504 days in the JJA season, there are some decreases in stickiness on extreme T_w days in the
505 Northern Hemisphere during DJF, when T_w is relatively low. We note that there is not an
506 equivalently large land mass below 40°S harboring cold, dry air (such as northern North
507 America or Eurasia) that could compare for the Southern Hemisphere in JJA. Spatial patterns
508 in the standard deviation of stickiness are similar for extreme T_w conditions under mean
509 conditions in both seasons, but the magnitude is generally lower during extreme events
510 (Figure S14b and S15b). Locations which exhibit low standard deviation in stickiness during
511 extreme humid heat events may provide insight into the important physical controls over
512 local extreme humid heat events.

513 The patterns described above are not directly observable by plotting the global dry
514 bulb temperature, specific humidity, or relative humidity associated with mean and extreme
515 humid heat events (Figures 7 and 8). All stations show both higher specific humidity and dry
516 bulb temperature on extreme humid heat days than during average humid heat conditions,
517 regardless of season. Some regions do exhibit decreases in local relative humidity on these
518 extreme humid heat days, such as Alaska, northern Europe, and southeast China. However,
519 these three locations all experience increases in stickiness during extreme humid heat days
520 compared to mean conditions (Figure S20). These extreme days associated with decreased
521 relative humidity but increased stickiness may stem from the disparity between the
522 exponential increase in saturation vapor pressure and the linear increase in stickiness
523 associated with elevated temperatures, a phenomenon originating ultimately from the
524 stickiness definition (Figure 4). Such events could be caused by flow from the continents' dry
525 interior or strong transient high pressure systems that could increase local dry bulb
526 temperatures without concomitantly increasing moisture sufficiently to maintain relative
527 humidity (Zscheischler & Seneviratne 2017). In contrast, during DJF seasonally high-humid
528 heat events, regions such as the western United States, central Europe, Eurasia, and eastern
529 China exhibit decreases in relative humidity while experiencing strong decreases in
530 stickiness. The seasonal differences in the relationship between relative humidity and
531 stickiness reflect the distinct seasonal climatologies in the Northern Hemisphere, as baseline
532 dry bulb temperatures are much higher in the summer than the winter.



533

534 **Figure 7:** Global maps of mean a) specific humidity, b) relative humidity, and c) temperature during hour
 535 of daily maximum T_w at each station location based on subset of the data record during JJA season. Each
 536 plot shows the difference between the conditions occurring during extreme T_w days compared to all days
 537 (analogous to the bottom panel of Figure 5).



539

540 **Figure 8:** Global maps of mean a) specific humidity, b) relative humidity, and c) temperature during hour
 541 of daily maximum T_w at each station location based on subset of the data record during DJF season. Each
 542 plot shows the difference between the conditions occurring during extreme T_w days compared to all days
 543 (analogous to the bottom panel of Figure 6).

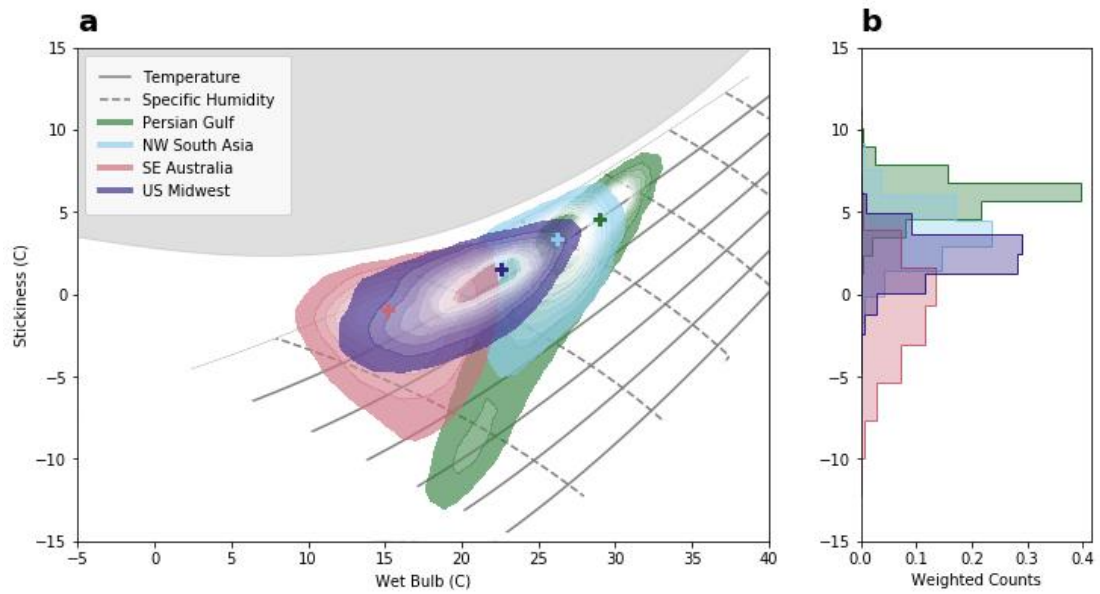
544

545 The spatial patterns in the difference in stickiness during mean versus extreme humid
 546 heat days are most similar to those of specific humidity, with the largest differences in
 547 regions such as the Persian Gulf and the Gulf of California (JJA) and the southeastern United
 548 States, the Sahel, and Australia (DJF) (Figures 7a and 8a). This similarity in spatial patterns
 549 between stickiness and specific humidity is again consistent with the Clausius-Clapeyron
 550 relationship. The nonlinear relationship between temperature and specific humidity suggests
 551 that at moderate-to-high temperatures, specific humidity fluctuations may be more critical
 552 than dry bulb temperature fluctuations to the achievement of extreme T_w values. Spatial
 553 patterns in specific humidity changes have thus been shown to drive those of humid heat
 554 (Lutsko 2021), which is reflected in global stickiness patterns. The key difference in the
 555 spatial pattern of these two variables is that while all stations exhibit higher specific humidity

556 during extreme T_w days than during average conditions, this is not the case for stickiness
557 (particularly in high northern latitudes during boreal winter). The magnitude of specific
558 humidity increases are comparable across much of each summer hemisphere, and can even
559 increase with latitude in regions such as the United States in JJA and Australia in DJF,
560 indicating the large intraseasonal variability at these latitudes.

561 Returning to the four case study regions and exploring the temporal variations in the
562 relationships between stickiness and humid heat further highlights the dependency of extreme
563 T_w on anomalous specific humidity (high stickiness). In each region, the highest recorded T_w
564 occur at the highest stickiness values, following along the saturation curve (Figure 9).
565 However, there is a large range in stickiness at locally defined moderate levels of humid heat,
566 particularly in the Persian Gulf and NW South Asia. At a threshold of 27°C , these two
567 regions experience a range of stickiness from about -1°C to 5°C . The larger range in
568 stickiness associated with moderately high T_w thresholds within these two individual regions
569 is consistent with the increased spatial variability in global stickiness at moderately high T_w
570 intensities (Figure 10). We note that 4,640 stations have experienced T_w thresholds between
571 $25\text{-}26^\circ\text{C}$ in their historical records, with a range of both negative and positive co-occurring
572 stickiness conditions. In contrast, only 1,982 stations have previously recorded T_w conditions
573 between $29\text{-}30^\circ\text{C}$, and the co-occurring stickiness is consistently higher, with an average
574 stickiness across stations of 5.2°C . In SE Australia and the US Midwest, low T_w conditions
575 are associated with relatively low dry bulb temperatures and increased stickiness. In these
576 mid-latitude (rather than subtropical) regions, jet stream variability may influence local
577 temperature and moisture conditions and drive these patterns (He et al. 2023). It is also
578 possible that vegetation cover within these regions helps supply moisture during the summer
579 months, preventing severely low specific humidity levels even as dry bulb temperatures drop.
580 The distinct summers of 2011 and 2012 in the US Midwest are examples illustrating the
581 range of stickiness at moderate T_w thresholds in this region. The hot and dry summer of 2012
582 was widely reported on due to the experience of flash droughts (e.g., Mallya et al. 2013;
583 Otkin et al. 2016). While the preceding summer only experienced moderate dry bulb
584 temperatures, observed T_w values throughout the region were actually higher than in 2012
585 (Figure S21). Stickiness can help to characterize the contrasting conditions that dominated
586 these summers – both in the bulk of the distribution and in the tails, as well as distinguishing
587 primarily temperature-driven versus primarily humidity-driven differences – without
588 resorting to combinations of other temperature and humidity variables.

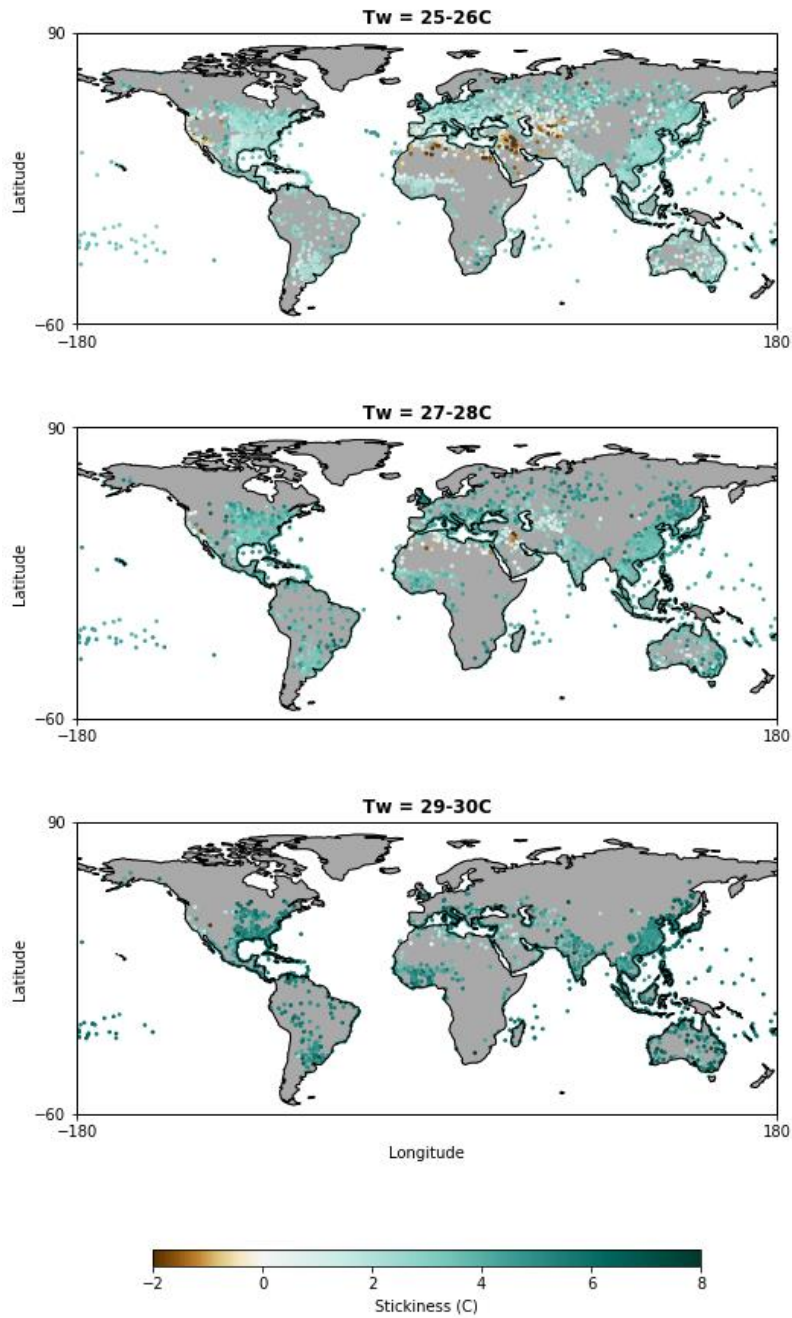
589



590

591 **Figure 9:** a) Daily T_w and stickiness occurring at the hour of daily maximum T_w for historical data record
592 over all stations in each region. Shaded contours indicate Gaussian kernel density estimations; gray solid
593 (dashed) contours indicate temperature (specific humidity) isopleths. Gray shading indicates conditions
594 producing supersaturated air. Shown for local summer season (JJA for the Persian Gulf, NW South Asia,
595 and the US Midwest; DJF for SE Australia). b) Stickiness distributions during 90th percentile T_w days in
596 each region.

597



598

599

600 **Figure 10:** Mean stickiness conditions during hour of daily maximum T_w of a specific threshold. Station
 601 locations are only plotted if the T_w threshold is surpassed in the historical record.

602

603 As discussed in the introduction, existing approaches to quantifying the temperature
 604 and humidity contributions to T_w extremes tend to be defined on scales that are specific to a
 605 given location and depend on the typical ranges in these variables that occur there. Stickiness
 606 aims to be more broadly relevant and allow greater ease of comparison between climates. In
 607 our view, stickiness is still most valuable in a somewhat relative sense, in that its variations
 608 are systematically different at different T_w values as shown above – in particular, very high

609 T_w tends to only occur concurrently with high stickiness, while stickiness varies more widely
610 at lower T_w . Stickiness provides the greatest insights into the physical drivers of extreme
611 humid heat when evaluating it at similar T_w values (i.e., along a vertical line in Figure 9).
612 Comparisons across very different regions and seasons reveal stickiness' inherent sensitivity
613 to baseline temperature, since the Clausius-Clapeyron relationship dictates that the latent heat
614 of a parcel increases faster than its dry enthalpy with temperature. This also implies that in
615 general under climate change, latent heat will contribute ever more to the total moist static
616 energy and related T_w (Matthews 2018; Lutsko 2021), increasing the fraction of global
617 extreme events with high stickiness.

618 However, in contrast to existing approaches, the utility of stickiness as a diagnostic is
619 not relative in the sense of depending on the range of variability within a given climate. It
620 need only be defined once, rather than many times for different locations, and comparing two
621 stickiness values occurring at the same T_w is meaningful even if the two observations were
622 taken from different locations with different ranges of seasonal or subseasonal variation. We
623 conclude that, while no single diagnostic meets all possible needs, stickiness may be a useful
624 addition to existing variables for analyses of the contributions of temperature and humidity to
625 variations in T_w or other measures of humid heat.

626

627 **4. Discussion and Conclusions**

628 While the relative dependence of humid heat on temperature and humidity varies
629 spatially and temporally across the globe, we find that extreme humid heat at thresholds
630 sufficiently high to impact human health tends to be humidity-dependent — that is,
631 associated with relatively large moisture anomalies rather than temperature anomalies. We
632 have demonstrated this phenomenon by examining the historical record of traditional metrics
633 such as dry bulb temperature, specific humidity, relative humidity, and saturation deficit
634 within a set of climatologically diverse case study regions. We also show that variation in this
635 dependence can be succinctly described using the newly derived variable stickiness, which
636 allows for the direct comparison of the varying dependencies of humid heat, both within one
637 location across time and at one time across the globe.

638 The global consistency of stickiness allows for the comparison of the potentially
639 unique regional dynamics leading to local humid heat extremes. We find that the difference
640 in stickiness between mean and extreme humid heat days has some common features across

641 the globe, homogeneous at local scales and heterogeneous at regional scales. Humid heat at
642 high magnitudes tends to be humidity-dependent (high stickiness). This is consistent with
643 recent literature investigating the dynamics of extreme events in humid heat hotspots,
644 highlighting key factors and processes such as moisture advection (Monteiro and Caballero
645 2019) and proximity to warm water bodies or irrigated land (Im et al. 2017; Mishra et al.
646 2020; Krakauer et al. 2020; Jha et al. 2022). The importance of such processes underscores
647 the influence of moisture modulation for driving humid heat extremes, especially when
648 paired with stability against deep convection (Raymond et al. 2021). We also find that
649 regions at high elevation including the areas “downwind” of mountain ranges all exhibit low
650 stickiness conditions during both mean and extreme humid heat days. While it is difficult for
651 T_w at high elevation to exceed dangerous thresholds for human health (Raymond et al. 2022),
652 these results highlight that the fluctuations in temperature in these relatively dry
653 environments are important to local T_w anomalies, in some cases via localized phenomena
654 such as downslope wind events (Gershunov et al. 2021). These patterns may become
655 increasingly important as populous cities at high elevation such as Denver, Colorado or
656 Kabul, Afghanistan begin to experience more heat extremes in the future (Coffel et al. 2019).

657 Stickiness also serves as an efficient and consistent quantitative metric to assess the
658 varying contributions from temperature and specific humidity towards humid heat events at
659 an individual location over time. The present study highlights the wide variation in the
660 temperature-vs-humidity contributions to moderate humid heat in many regions, in agreement
661 with regionally specific studies in locations such as the Persian Gulf, South Asia, China, and
662 the United States (Ivanovich et al. 2022; Wang et al. 2019; Raymond et al. 2017). Large scale
663 modes of climate variability such as the El Niño Southern Oscillation, the Madden-Julian
664 Oscillation, and the Boreal Summer Intraseasonal Oscillation have been shown to influence
665 extreme humid heat across the globe (Ivanovich et al. 2022; Speizer et al. 2022) and may
666 contribute to the high variability in stickiness observed in regions such as the Sahel.
667 Variability may also be influenced directly by changes in sea surface temperature,
668 particularly in regions such as South Africa in close proximity to the Agulhas Current
669 (Rouault et al. 2002). In southeast Australia, high variability may be strongly influenced by
670 wind direction on a variety of timescales, whether by synoptic scale disturbances or seasonal
671 monsoon circulation, and associated moisture transport (Watterson 2001).

672 The capacity of stickiness to quantify the contribution of temperature and specific
673 humidity towards humid heat extremes may help locations identify which variables are most

674 important to predicting the local occurrence of heat stress. There is ongoing debate
675 concerning the physiological expectation that humidity is an important factor for the
676 experience of human heat stress (Mora et al. 2017; Parsons 2006; Steadman 1979; Fanger
677 1970) versus the lack of epidemiological evidence that high humidity helps to predict human
678 mortality and morbidity compared to dry bulb temperature alone (Armstrong et al. 2019;
679 Vaneckova et al. 2011; Barnett et al. 2010). One challenge which may contribute to this
680 disagreement is that locations where we might expect a low correlation between extreme dry
681 and humid heat days (i.e., locations where humid heat may provide additional predictive skill
682 compared to dry temperatures) rarely overlap with locations with available and reliable
683 human health data (Baldwin et al. 2023). Places with high variability in stickiness during
684 local warm periods could point to regions where the differential impacts of extreme dry and
685 humid heat on human health may be more easily separated, should the necessary human
686 health data be available. In regions that exhibit either high variability in stickiness or
687 consistently high stickiness, communicating heat stress risk using a heat stress metric rather
688 than dry bulb temperature alone may be essential for the most effective local extreme event
689 preparedness. Identifying regions with consistently negative stickiness may also offer
690 insights. In such regions, humid heat extremes tend to occur in the presence of elevated dry
691 bulb temperatures. Traditional metrics of tracking heat stress based on dry bulb temperature
692 alone or more temperature-dependent heat stress metrics (e.g., Heat Index) may be sufficient
693 in these locations to identify future extreme heat stress days. Given that the interpretation of
694 results and translation into adaptation methods depends strongly on the heat stress metric
695 selected (Simpson et al. 2023), introducing stickiness as offering an additional perspective on
696 these disagreements may be helpful, in combination with other metrics. Such explorations
697 using stickiness should also consider the influence of physiological health and climate
698 acclimatization on individuals' experience of heat stress, which can inform regional
699 applications of the variable. Knowing the local shape of the stickiness distribution in a region
700 may also help to forecast when an individual meteorological event may or may not pose a
701 threat of extreme humid heat. For example, in the Persian Gulf where humid heat extremes
702 tend to have high stickiness, a high pressure system that increases local temperatures may not
703 be as detrimental as the stalling of summer winds over the Gulf waters which allows for the
704 buildup of moisture along the coast (Ivanovich et al. 2022; Raymond et al. 2021). In the
705 current analysis, we do not differentiate between variability driven by interannual or intra-
706 annual changes and hypothesize that both may play an important role in local stickiness
707 variability.

708 Distinguishing between humid heat driven by anomalous temperature and humidity
709 through the use of metrics such as stickiness helps to prepare for the unique impacts of each
710 type of extreme. Most heat stress studies have examined T_w above a certain threshold, such as
711 the local 99th percentile or a fixed 35°C value. However, Vecellio et al. (2021) found that for
712 a fixed T_w , less moist humid heat is in fact significantly more dangerous to human health, due
713 primarily to physiological limitations on sweat rates. As a result, identifying locations which
714 experience moderately high T_w and low stickiness, such as the southwest United States, may
715 improve the ability of climate studies to address heat stress risks that are not typically
716 identified by considering T_w or other traditional heat stress metrics alone (Simpson et al.
717 2023; Vanos et al. 2020). Additionally, crop productivity effects due to increased vapor
718 pressure deficit, or increased risk of wildfire at high temperatures and low humidity, indicates
719 that low stickiness may be worse for plant health (Ting et al. 2023). Future work could
720 compare stickiness conditions to crop productivity data or wildfire occurrence to test these
721 relationships explicitly. Stickiness variability also affects the local implications for humid
722 heat of practices such as irrigation, which have been shown to increase local humidity
723 conditions and trigger extreme humid heat (Jha et al. 2022; Krakauer et al. 2020; Mishra et al.
724 2020; Monteiro and Caballero 2019). While irrigation has been shown to reduce local dry
725 heat conditions, the local increases in humidity can often compensate and increase humid
726 heat conditions. Particularly in regions where economic livelihoods depend on agricultural
727 labor, considering current conditions and the possible tradeoffs of these changes is essential.

728 The potential future extensions of this research range from dynamical to impacts-
729 focused. Here we explore the subseasonal variability of stickiness in each of the case study
730 regions by plotting the full records for the JJA and DJF seasons using daily scale data.
731 Identifying extreme humid heat events from each of these regions and exploring the temporal
732 evolution of stickiness on hourly timescales could elucidate specific physical mechanisms.
733 For example, tracking the evolution of stickiness throughout the duration of meteorological
734 events such as a thunderstorm while considering the simultaneous influence of the local
735 background climate, vegetation, and urbanization could shed light upon the dynamics of
736 these events and the potential for compound extremes. Future applications of this work could
737 also investigate the modulation of extreme dry and humid heat by vegetation cover. As
738 demonstrated by the distinction between global patterns of stickiness compared to
739 temperature and specific humidity alone, utilizing stickiness could help to evaluate how
740 vegetation cover might influence potential constraints on both dry bulb temperatures and

741 vapor pressure deficits in locations such as the US Midwest by increasing local surface level
742 moisture. The presence of dense vegetation in this midlatitude region could serve as a
743 mediator to limit extreme dry bulb temperatures and vapor pressure deficits, helping to buffer
744 any potential threats to crop productivity associated with high canopy dry bulb temperatures
745 (Mueller et al. 2016). Future work should also explore the influence of dataset uncertainties
746 as well as how stickiness interacts with the non-climate dimensions of heat stress impacts,
747 such as how access to artificial cooling and the amount of strenuous outdoor activity could
748 shift with heat hazards and stickiness variations. Finally, additional research could attempt
749 extensions our derivation of stickiness by quantifying the contributions towards humid heat
750 from other climate variables known to influence human health, such as solar insolation and
751 wind speed (Buzan et al. 2015).

752 As climate change continues to affect land-ocean contrasts and atmospheric
753 circulation, in addition to other factors such as urbanization, deforestation, and agricultural
754 land-use patterns, local stickiness conditions may shift. Further research should consider how
755 future changes in global temperature and moisture patterns will influence the types of humid
756 heat extremes and inform how to best prepare for their distinct societal impacts. In speaking
757 to both atmospheric physics and public health impacts, stickiness provides a uniquely holistic
758 approach for characterizing the spatial and temporal diversity of extreme humid heat events.

759

760 *Acknowledgments.*

761 Funding for C. Ivanovich and R. Horton was provided by National Oceanic and Atmospheric
762 Administration's Regional Integrated Sciences and Assessments program, Grant
763 NA15OAR4310147. A portion of C. Raymond's work was carried out at the Jet Propulsion
764 Laboratory, California Institute of Technology, under a contract with the National
765 Aeronautics and Space Administration (80NM0018D0004). A. H. Sobel acknowledges
766 support from NSF Grant AGS-1758603. The authors declare no conflicts of interest with
767 regard to this research. We thank Marc Spiegelman for his advice on mathematical questions
768 that came up in the derivation of stickiness.

769

770 *Data Availability Statement.*

771 All datasets used in this analysis are publicly accessible via the following websites: HadISD,
772 <https://www.metoffice.gov.uk/hadobs/hadisd/>; and ERA5,
773 <https://www.ecmwf.int/en/forecasts/datasets/reanalysis-datasets/era5>. All code used for the
774 derivations, calculations, and data visualization will be publicly available on Github upon
775 manuscript publication.

776

777

REFERENCES

778 Abatzoglou, J. T., & Williams, A. P. (2016). Impact of anthropogenic climate change on
779 wildfire across western US forests. *Proceedings of the National Academy of Sciences*,
780 *113*(42), 11770–11775. <https://doi.org/10.1073/pnas.1607171113>

781 Barnett, A. G., et al. “What Measure of Temperature Is the Best Predictor of Mortality?”
782 *Environmental Research*, vol. 110, no. 6, Aug. 2010, pp. 604–11,
783 <https://doi.org/10.1016/j.envres.2010.05.006>.

784 Bohren, C. F., & Albrecht, B. A. (1998). *Atmospheric thermodynamics*. New York: Oxford
785 University Press.

786 Bowman, D. M. J. S., Balch, J. K., Artaxo, P., Bond, W. J., Carlson, J. M., Cochrane, M. A.,
787 et al. (2009). Fire in the Earth System. *Science*, *324*(5926), 481–484.
788 <https://doi.org/10.1126/science.1163886>

789 Buzan, J. R., Oleson, K., & Huber, M. (2015). Implementation and comparison of a suite of
790 heat stress metrics within the Community Land Model version 4.5. *Geoscientific*
791 *Model Development*, *8*(2), 151–170. <https://doi.org/10.5194/gmd-8-151-2015>

792 Buzan, Jonathan R., & Huber, M. (2020). Moist Heat Stress on a Hotter Earth. *Annual*
793 *Review of Earth and Planetary Sciences*, *48*(1), 623–655.
794 <https://doi.org/10.1146/annurev-earth-053018-060100>

795 Coffel, E. D., Horton, R. M., & de Sherbinin, A. (2018). Temperature and humidity based
796 projections of a rapid rise in global heat stress exposure during the 21st century.
797 *Environmental Research Letters*, *13*(1), 014001. [https://doi.org/10.1088/1748-](https://doi.org/10.1088/1748-9326/aaa00e)
798 [9326/aaa00e](https://doi.org/10.1088/1748-9326/aaa00e)

799 Coffel, E. D., Lesk, C., Winter, J. M., Osterberg, E. C., & Mankin, J. S. (2022). Crop-climate
800 feedbacks boost US maize and soy yields. *Environmental Research Letters*, *17*(2),
801 024012. <https://doi.org/10.1088/1748-9326/ac4aa0>

802 Chakraborty, T., Venter, Z. S., Qian, Y., & Lee, X. (2022). Lower Urban Humidity
803 Moderates Outdoor Heat Stress. *AGU Advances*, 3(5).
804 <https://doi.org/10.1029/2022AV000729>

805 Dai, A. (2006). Recent Climatology, Variability, and Trends in Global Surface Humidity.
806 *Journal of Climate*, 19(15), 3589–3606. <https://doi.org/10.1175/JCLI3816.1>

807 Davies-Jones, R. (2008). An Efficient and Accurate Method for Computing the Wet-Bulb
808 Temperature along Pseudoadiabats. *Monthly Weather Review*, 136(7), 2764–2785.
809 <https://doi.org/10.1175/2007MWR2224>.

810 Dunn, R. J. H. (2019). HadISD version 3: monthly updates. *Hadley Centre Technical Note*.

811 Dunn, R. J. H., Willett, K. M., Thorne, P. W., Woolley, E. V., Durre, I., Dai, A., et al. (2012).
812 HadISD: a quality-controlled global synoptic report database for selected variables at
813 long-term stations from 1973–2011. *Climate of the Past*, 8(5), 1649–1679.
814 <https://doi.org/10.5194/cp-8-1649-2012>

815 Ebi, K. L., Capon, A., Berry, P., Broderick, C., De Dear, R., Havenith, G., et al. (2021). Hot
816 weather and heat extremes: health risks. *The Lancet*, 398(10301), 698–708.
817 [https://doi.org/10.1016/S0140-6736\(21\)01208-3](https://doi.org/10.1016/S0140-6736(21)01208-3)

818 Fanger, P. O. (1970). *Thermal Comfort: Analysis and Applications in Environmental*
819 *Engineering*. Danish Technical Press.

820 Flament, P. (2002). A state variable for characterizing water masses and their diffusive
821 stability: spiciness. *Progress in Oceanography*, 54(1–4), 493–501.
822 [https://doi.org/10.1016/S0079-6611\(02\)00065-4](https://doi.org/10.1016/S0079-6611(02)00065-4)

823 Gershunov, A., Guzman Morales, J., Hatchett, B., Guirguis, K., Aguilera, R., Shulgina, T., et
824 al. (2021). Hot and cold flavors of southern California’s Santa Ana winds: their
825 causes, trends, and links with wildfire. *Climate Dynamics*, 57(7–8), 2233–2248.
826 <https://doi.org/10.1007/s00382-021-05802-z>

827 Griffiths, D. F., & Watson, G. A. (1996). *Numerical Analysis 1995*. CRC Press.

828 He, Y., Zhu, X., Sheng, Z., & He, M. (2023). Resonant Waves Play an Important Role in the
829 Increasing Heat Waves in Northern Hemisphere Mid-Latitudes Under Global
830 Warming. *Geophysical Research Letters*, 50(14), e2023GL104839.
831 <https://doi.org/10.1029/2023GL104839>

- 832 Hersbach, H., Bell, B., Berrisford, P., Hirahara, S., Horányi, A., Muñoz-Sabater, J., et al.
833 (2020). The ERA5 global reanalysis. *Quarterly Journal of the Royal Meteorological*
834 *Society*, 146(730), 1999–2049. <https://doi.org/10.1002/qj.3803>
- 835 Horton, R. M., Mankin, J. S., Lesk, C., Coffel, E., & Raymond, C. (2016). A Review of
836 Recent Advances in Research on Extreme Heat Events. *Current Climate Change*
837 *Reports*, 2(4), 242–259. <https://doi.org/10.1007/s40641-016-0042-x>
- 838 Im, E.-S., Pal, J. S., & Eltahir, E. A. B. (2017). Deadly heat waves projected in the densely
839 populated agricultural regions of South Asia. *Science Advances*, 3(8), e1603322.
840 <https://doi.org/10.1126/sciadv.1603322>
- 841 Ivanovich, C., Anderson, W., Horton, R., Raymond, C., & Sobel, A. (2022). The Influence of
842 Intraseasonal Oscillations on Humid Heat in the Persian Gulf and South Asia. *Journal*
843 *of Climate*, 35(13), 4309–4329. <https://doi.org/10.1175/JCLI-D-21-0488.1>
- 844 Jha, R., Mondal, A., Devanand, A., Roxy, M. K., & Ghosh, S. (2022). Limited influence of
845 irrigation on pre-monsoon heat stress in the Indo-Gangetic Plain. *Nature*
846 *Communications*, 13(1), 4275. <https://doi.org/10.1038/s41467-022-31962-5>
- 847 Kovats, R. S., & Hajat, S. (2008). Heat Stress and Public Health: A Critical Review. *Annual*
848 *Review of Public Health*, 29(1), 41–55.
849 <https://doi.org/10.1146/annurev.publhealth.29.020907.090843>
- 850 Krakauer, Nir Y., et al. “Effect of Irrigation on Humid Heat Extremes.” *Environmental*
851 *Research Letters*, vol. 15, no. 9, Sept. 2020, p. 094010, [https://doi.org/10.1088/1748-](https://doi.org/10.1088/1748-9326/ab9ecf)
852 [9326/ab9ecf](https://doi.org/10.1088/1748-9326/ab9ecf).
- 853 Lu, Y.-C., & Romps, D. M. (2023). Is a wet-bulb temperature of 35 ° C the correct threshold
854 for human survivability? *Environmental Research Letters*, 18(9), 094021.
855 <https://doi.org/10.1088/1748-9326/ace83c>
- 856 Lutsko, N. J. (2021). The Relative Contributions of Temperature and Moisture to Heat Stress
857 Changes under Warming. *Journal of Climate*, 34(3), 901–917.
858 <https://doi.org/10.1175/JCLI-D-20-0262.1>
- 859 Mallya, G., et al. “2012 Midwest Drought in the United States.” *Journal of Hydrologic*
860 *Engineering*, vol. 18, no. 7, 2013, pp. 737–45,
861 [https://doi.org/10.1061/\(ASCE\)HE.1943-5584.0000786](https://doi.org/10.1061/(ASCE)HE.1943-5584.0000786).

- 862 Masterton, J. M., & Richardson, F. A. (1979). *Humidex ; a method of quantifying human*
863 *discomfort due to excessive heat and humidity*. Downsview, Ont.: Environment
864 Canada, Atmospheric Environment. Retrieved from [https://bac-](https://bac-lac.on.worldcat.org/oclc/1032942635)
865 [lac.on.worldcat.org/oclc/1032942635](https://bac-lac.on.worldcat.org/oclc/1032942635)
- 866 Matthews, T. (2018). Humid heat and climate change. *Prog. Phys. Geog.*, 42 (3), 391-405.
867 <https://doi.org/10.1177/0309133318776490>.
- 868 Mishra, V., Ambika, A. K., Asoka, A., Aadhar, S., Buzan, J., Kumar, R., & Huber, M.
869 (2020). Moist heat stress extremes in India enhanced by irrigation. *Nature*
870 *Geoscience*, 13(11), 722–728. <https://doi.org/10.1038/s41561-020-00650-8>
- 871 Monteiro, J. M., & Caballero, R. (2019). Characterization of Extreme Wet-Bulb Temperature
872 Events in Southern Pakistan. *Geophysical Research Letters*, 46(17–18), 10659–
873 10668. <https://doi.org/10.1029/2019GL084711>
- 874 Mora, C., Dousset, B., Caldwell, I. R., Powell, F. E., Geronimo, R. C., Bielecki, C. R., et al.
875 (2017). Global risk of deadly heat. *Nature Climate Change*, 7(7), 501–506.
876 <https://doi.org/10.1038/nclimate3322>
- 877 Mueller, N. D., Butler, E. E., McKinnon, K. A., Rhines, A., Tingley, M., Holbrook, N. M., &
878 Huybers, P. (2016). Cooling of US Midwest summer temperature extremes from
879 cropland intensification. *Nature Climate Change*, 6(3), 317–322.
880 <https://doi.org/10.1038/nclimate2825>
- 881 Nelder, J. A., & Mead, R. (1965). A Simplex Method for Function Minimization. *The*
882 *Computer Journal*, 7(4), 308–313. <https://doi.org/10.1093/comjnl/7.4.308>
- 883 Otkin, Jason A., et al. “Assessing the Evolution of Soil Moisture and Vegetation Conditions
884 during the 2012 United States Flash Drought.” *Agricultural and Forest Meteorology*,
885 vol. 218–219, Mar. 2016, pp. 230–42,
886 <https://doi.org/10.1016/j.agrformet.2015.12.065>.
- 887 Pal, J. S., & Eltahir, E. A. B. (2016). Future temperature in southwest Asia projected to
888 exceed a threshold for human adaptability. *Nature Climate Change*, 6(2), 197–200.
889 <https://doi.org/10.1038/nclimate2833>
- 890 Parsons, K. (2006). Heat Stress Standard ISO 7243 and its Global Application. *Industrial*
891 *Health*, 44(3), 368–379. <https://doi.org/10.2486/indhealth.44.368>

- 892 Photiadou, C., Jones, M., Keellings, D., & Dewes, C. (2014). Modeling European hot spells
893 using extreme value analysis. *Climate Research*, 58(3), 193–207.
894 <https://doi.org/10.3354/cr01191>
- 895 Raymond, C., Singh, D., & Horton, R. M. (2017). Spatiotemporal Patterns and Synoptics of
896 Extreme Wet-Bulb Temperature in the Contiguous United States: U.S. Extreme-WBT
897 Patterns. *Journal of Geophysical Research: Atmospheres*, 122(24), 13,108-13,124.
898 <https://doi.org/10.1002/2017JD027140>
- 899 Raymond, Colin, Matthews, T., & Horton, R. M. (2020). The emergence of heat and
900 humidity too severe for human tolerance. *Science Advances*, 6(19), eaaw1838.
901 <https://doi.org/10.1126/sciadv.aaw1838>
- 902 Raymond, Colin, Matthews, T., Horton, R. M., Fischer, E. M., Fueglistaler, S., Ivanovich, C.,
903 et al. (2021). On the Controlling Factors for Globally Extreme Humid Heat.
904 *Geophysical Research Letters*, 48(23). <https://doi.org/10.1029/2021GL096082>
- 905 Raymond, C., Waliser, D., Guan, B., Lee, H., Loikith, P., Massoud, E., et al. (2022).
906 Regional and Elevational Patterns of Extreme Heat Stress Change in the US.
907 *Environmental Research Letters*. <https://doi.org/10.1088/1748-9326/ac7343>
- 908 Rogers, C. D. W., Ting, M., Li, C., Kornhuber, K., Coffel, E. D., Horton, R. M., et al. (2021).
909 Recent Increases in Exposure to Extreme Humid-Heat Events Disproportionately
910 Affect Populated Regions. *Geophysical Research Letters*, 48(19).
911 <https://doi.org/10.1029/2021GL094183>
- 912 Röthlisberger, M., & Papritz, L. (2023). A Global Quantification of the Physical Processes
913 Leading to Near-Surface Cold Extremes. *Geophysical Research Letters*, 50(5).
914 <https://doi.org/10.1029/2022GL101670>
- 915 Rouault, M., White, S. A., Reason, C. J. C., Lutjeharms, J. R. E., & Jobard, I. (2002). Ocean–
916 Atmosphere Interaction in the Agulhas Current Region and a South African Extreme
917 Weather Event. *Weather and Forecasting*, 17(4), 655–669.
918 [https://doi.org/10.1175/1520-0434\(2002\)017<0655:OAITA>2.0.CO;2](https://doi.org/10.1175/1520-0434(2002)017<0655:OAITA>2.0.CO;2)
- 919 Schauburger, B., Archontoulis, S., Arneeth, A., Balkovic, J., Ciais, P., Deryng, D., et al.
920 (2017). Consistent negative response of US crops to high temperatures in
921 observations and crop models. *Nature Communications*, 8(1), 13931.
922 <https://doi.org/10.1038/ncomms13931>

- 923 Sherwood, S. C., & Huber, M. (2010). An adaptability limit to climate change due to heat
924 stress. *Proceedings of the National Academy of Sciences*, *107*(21), 9552–9555.
925 <https://doi.org/10.1073/pnas.0913352107>
- 926 Simpson, Charles H., et al. “Commonly Used Indices Disagree about the Effect of Moisture
927 on Heat Stress.” *Npj Climate and Atmospheric Science*, vol. 6, no. 1, July 2023, pp.
928 1–7, <https://doi.org/10.1038/s41612-023-00408-0>.
- 929 Speizer, S., Raymond, C., Ivanovich, C., & Horton, R. M. (2022). Concentrated and
930 Intensifying Humid Heat Extremes in the IPCC AR6 Regions. *Geophysical Research*
931 *Letters*, *49*(5). <https://doi.org/10.1029/2021GL097261>
- 932 Steadman, R. G. (1979). The Assessment of Sultriness. Part I: A Temperature-Humidity
933 Index Based on Human Physiology and Clothing Science. *Journal of Applied*
934 *Meteorology and Climatology*, *18*(7), 861–873. [https://doi.org/10.1175/1520-0450\(1979\)018<0861:TAOSPI>2.0.CO;2](https://doi.org/10.1175/1520-0450(1979)018<0861:TAOSPI>2.0.CO;2)
- 936 Tan, J., Zheng, Y., Tang, X., Guo, C., Li, L., Song, G., et al. (2010). The urban heat island
937 and its impact on heat waves and human health in Shanghai. *International Journal of*
938 *Biometeorology*, *54*(1), 75–84. <https://doi.org/10.1007/s00484-009-0256-x>
- 939 Ting, M., Lesk, C., Liu, C., Li, C., Horton, R. M., Coffel, E. D., et al. (2023). Contrasting
940 impacts of dry versus humid heat on US corn and soybean yields. *Scientific Reports*,
941 *13*(1), 710. <https://doi.org/10.1038/s41598-023-27931-7>
- 942 Vanos, J., Guzman-Echavarria, G., Baldwin, J. W., Bongers, C., Ebi, K. L., & Jay, O. (2023).
943 A physiological approach for assessing human survivability and liveability to heat in
944 a changing climate. *Nature Communications*, *14*(1), 7653.
945 <https://doi.org/10.1038/s41467-023-43121-5>
- 946 Vanos, J. K., Baldwin, J. W., Jay, O., & Ebi, K. L. (2020). Simplicity lacks robustness when
947 projecting heat-health outcomes in a changing climate. *Nature Communications*,
948 *11*(1), 6079. <https://doi.org/10.1038/s41467-020-19994-1>
- 949 Vaneckova, Pavla, et al. “Do Biometeorological Indices Improve Modeling Outcomes of
950 Heat-Related Mortality?” *Journal of Applied Meteorology and Climatology*, vol. 50,
951 no. 6, June 2011, pp. 1165–76, <https://doi.org/10.1175/2011JAMC2632.1>.
- 952 Vecellio, D. J., Wolf, S. T., Cottle, R. M., & Kenney, W. L. (2022). Evaluating the 35°C wet-
953 bulb temperature adaptability threshold for young, healthy subjects (PSU HEAT

- 954 Project). *Journal of Applied Physiology*, 132(2), 340–345.
955 <https://doi.org/10.1152/jappphysiol.00738.2021>
- 956 Wang, P., Leung, L. R., Lu, J., Song, F., & Tang, J. (2019). Extreme Wet-Bulb Temperatures
957 in China: The Significant Role of Moisture. *Journal of Geophysical Research:*
958 *Atmospheres*, 124(22), 11944–11960. <https://doi.org/10.1029/2019JD031477>
- 959 Wang, P., Yang, Y., Tang, J., Leung, L. R., & Liao, H. (2021). Intensified Humid Heat
960 Events Under Global Warming. *Geophysical Research Letters*, 48(2).
961 <https://doi.org/10.1029/2020GL091462>
- 962 Watterson, I. G. (2001). Wind-Induced Rainfall and Surface Temperature Anomalies in the
963 Australian Region. *Journal of Climate*, 14(9), 1901–1922.
964 [https://doi.org/10.1175/1520-0442\(2001\)014<1901:WIRAST>2.0.CO;2](https://doi.org/10.1175/1520-0442(2001)014<1901:WIRAST>2.0.CO;2)
- 965 Xue, P., & Eltahir, E. A. B. (2015). Estimation of the Heat and Water Budgets of the Persian
966 (Arabian) Gulf Using a Regional Climate Model*,+. *Journal of Climate*, 28(13),
967 5041–5062. <https://doi.org/10.1175/JCLI-D-14-00189.1>
- 968 Zscheischler, J., Martius, O., Westra, S., Bevacqua, E., Raymond, C., Horton, R. M., et al.
969 (2020). A typology of compound weather and climate events. *Nature Reviews Earth*
970 *& Environment*, 1(7), 333–347. <https://doi.org/10.1038/s43017-020-0060-z>

971

972

KEYWORDS

973 heat wave, humidity, climate, climate variability, extreme events